Journal of The Electrochemical Society, **154** (12) H1041-H1046 (2007)
0013-4651/2007/154(12)/H1041/6/$20.00 © The Electrochemical Society

Liquid-Phase Deposition of Al_2O_3 Thin Films on GaN

Sarbani Basu, Pramod K. Singh, Jian-Jiun Huang, and Yeong-Her Wang[z]

Department of Electrical Engineering, Institute of Microelectronics, Advanced Optoelectronic Technology Center, National Cheng Kung University, Tainan 701, Taiwan

Thin films of aluminum oxide (Al_2O_3) on GaN substrates were grown by the process of low-temperature liquid-phase deposition (LPD), in which aluminum sulfate with crystallized water [$Al_2(SO_4)_3 \cdot 18H_2O$] and sodium bicarbonate [$NaHCO_3$] were used as the precursors. The pH value of the growth solution plays an important role in the deposition process. The best quality of the oxide thin film was obtained at the pH value of 3.80, while the growth rate was 35 nm/h at the optimized concentration values of $Al_2(SO_4)_3$ = 0.0834 mol/L and $NaHCO_3$ = 0.211 mol/L and at the temperature of 30°C. The films were characterized by means of X-ray photoelectron spectroscopy, Auger electron spectroscopy, and atomic force microscopy. It was found that the leakage current density of 50 nm thin Al_2O_3 oxide film was between 10^{-4} and 10^{-5} A/cm^2 at a negative electric field of 1 MV/cm, with the breakdown electric field being greater than 10 MV/cm. After annealing the oxide at 750°C for 30 min, the leakage current density was lowered to the value of 10^{-6}–10^{-7} A/cm^2 at the negative electric field of 1 MV/cm. The oxide-semiconductor interface state density as calculated from the capacitance-voltage curve was 3.89×10^{11} cm^{-2} eV^{-1}.
© 2007 The Electrochemical Society. [DOI: 10.1149/1.2793700] All rights reserved.

Manuscript submitted January 16, 2007; revised manuscript received August 13, 2007. Available electronically October 22, 2007.

Much attention has been focused on replacing SiO_2 with Al_2O_3 as a dielectric insulation film for semiconductor device applications due to the latter's large bandgap (~9 eV), higher dielectric constant (k = 10), high breakdown electric field (5–10 MV cm^{-1}), good thermal stability (amorphous condition up to 1000°C), chemical stability against AlGaN (without interdiffusion and interaction of Si and Al), and lower lattice mismatch to GaN. An amorphous Al_2O_3 film shows a better barrier for alkali ions, impurities,[1] and higher radiation resistances. Because of these properties, ultrathin alumina films of nanometer scale are widely used as high-k material to replace SiO_2 in microelectronic devices such as dynamic random access memories (DRAMs)[2] and metal-oxide semiconductor field effect transistors (MOSFETs) based on both Si and III-V compound semiconductors.[3] Applications of Al_2O_3 films are also being investigated in a variety of other areas including in optics, solid-state electronics, and microelectromechanical systems (MEMS). In this study, our aim was to deposit a thin Al_2O_3 insulating layer for GaN metal oxide semiconductor high electron mobility transistor (MOSHEMT) device application to reduce the gate leakage current. Many conventional methods for fabricating Al_2O_3 films are described in different papers, including thermal oxidation,[4] metallorganic chemical vapor phase deposition (MOCVD),[5] direct-current reactive magnetron sputtering,[6] photoluminescent alumina films by pyrosol process,[7] and atomic layer deposition (ALD).[8]

The growth of Al_2O_3 thin films as achieved by the above-mentioned techniques involves high substrate temperatures (>750°C). This causes thermal strain and defect states in the semiconductor oxide interface, which in turn degrade device performance. The present work is a new attempt to deposit amorphous Al_2O_3 thin films on GaN substrates by means of the liquid phase deposition (LPD) method at low temperatures in order to avoid thermal strain and defects. This technique is found to incur low cost and is reliable and efficient. In our previous work, we have successfully demonstrated the deposition of a SiO_2 thin film on a GaN substrate by means of the LPD process at room temperature.[9]

Recently, Sun et al.[10] described the SiO_2 and Al_2O_3 thin films grown by LPD on GaAs and Si substrates; however, the aluminum–oxygen (Al–O) bonding spectra of the grown film was not identified by the X-ray photoelectron spectroscopy (XPS) study and the electrical characteristics were not given. In the current research, we therefore introduced a successful deposition of Al_2O_3 thin film on a GaN substrate with material and electrical characterization.

Experimental

This LPD deposition system[9] contains a temperature-controlled water bath that offers a uniform deposition temperature with ±0.1°C accuracy, a substrate holder, a Teflon beaker, a magnetic stirrer for the high homogeneity of the growth solution, a pH meter, a Teflon filter (0.1 μm), and an ultrasonic cleaner. The GaN epitaxial layer (2 μm) grown by MOCVD on a c-plane sapphire was used as the substrate for the Al_2O_3 thin-film deposition. The substrates were cleaned successively with acetone, methanol, and deionized (DI) water by sonicating each for 10 min and immersing them in hydrofluoric acid (HF) solution (1:1) for 1 min in order to remove the organic contaminants and native oxides of GaN. Aluminum sulfate [$Al_2(SO_4)_3 \cdot 18H_2O$] was placed in a Teflon beaker, and a small amount of water was added to form a nearly saturated solution of $Al_2(SO_4)_3$ as a source liquid. Then, sodium bicarbonate fine powder (as a deposition rate controller) was added slowly to obtain a pH value of 2.89 for the growth solution. After the addition of $NaHCO_3$, the hydrolysis of Al^{3+} particles and the concentration of $Al(OH)_3$ colloid particles increased, but no precipitation of the $Al(OH)_3$ particles was observed because the pH value was still low enough at 2.89.[11] An aluminum sulfate solution is strongly acidic due to Al^{+3} ions, and it reacts with sodium bicarbonate powder, thereby generating carbon dioxide bubbles. As soon as the reaction was completed, DI water was immediately added in order to increase the pH value to 3.80, which is the optimized pH value used for the deposition of an alumina film. The final growth solution of the $Al(OH)_3$ solution was produced by the electrolytes of $Al_2(SO_4)_3$ and Na_2SO_4. The solution was diluted at the proper time so that no precipitation occurred due to the crystallization of double sulfate [composed of Na_2SO_4 and $Al_2(SO_4)_3$]. The growth solution was transparent, and all the parameters were optimized with $Al_2(SO_4)_3$ = 0.0834 mol/L and $NaHCO_3$ = 0.211 mol/L (final concentrations). The solution was filtered through a 0.1 μm filter and was used for the film growth on GaN substrates by means of the immersion method. In this mechanism, $Al(OH)_3$ dissolved in acid when pH < 3.4 by generating Al^{+3} ions as well as in alkali when pH > 11 by generating $Al(OH)_4^-$ ions, but it remained undissolved when the pH value was between 4 and 10.[11] The precursor species $Al_2(SO_4)_3$ and $NaHCO_3$ were hydrolyzed and deposited on a clean GaN substrate. The Al_2O_3 films were prepared on the GaN substrate by the dehydration of aluminum hydroxide.[12] Postgrowth annealing was done to make the films denser.

The chemical reaction of film growth can be described in the following

$$Al_2(SO_4)_3 + 6NaHCO_3 \xrightarrow{\Delta} 2Al(OH)_3 + 3Na_2SO_4 + 6CO_2\uparrow$$

[z] E-mail: yhw@eembox.ncku.edu.tw

Downloaded on 2014-12-17 to IP 169.230.243.252 address. Redistribution subject to ECS terms of use (see ecsdl.org/site/terms_use) unless CC License in place (see abstract).

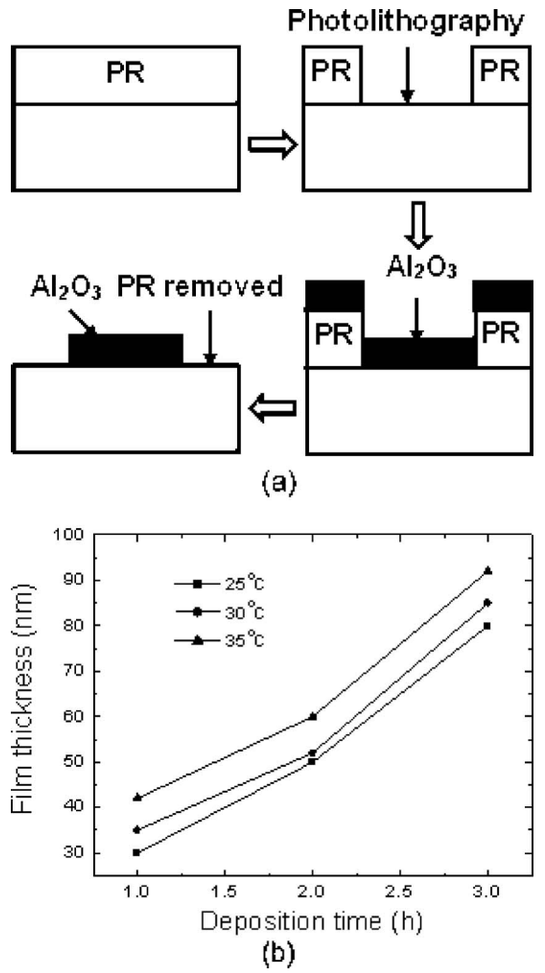

Figure 1. (a) Schematic of selective oxide growth and (b) film thickness vs deposition time.

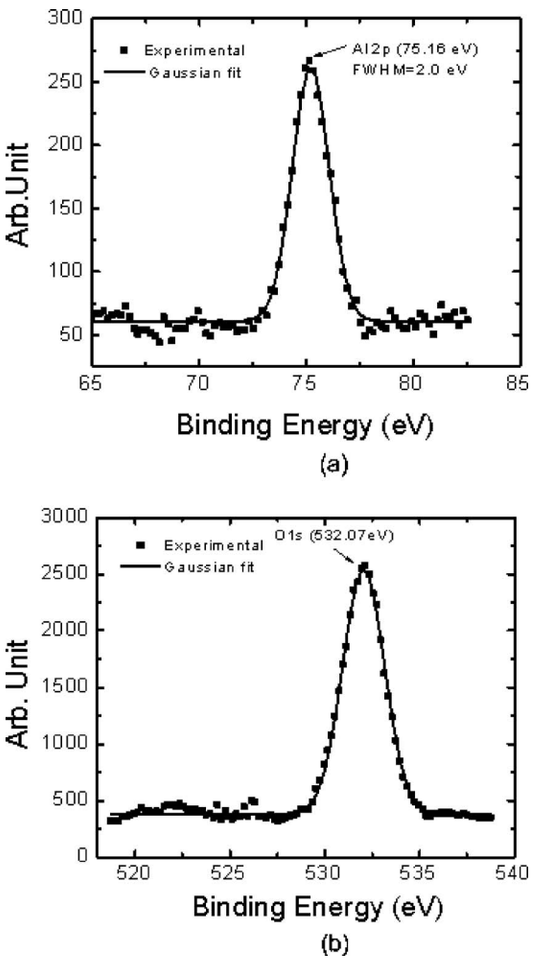

Figure 2. XPS spectra of a 70 nm thin Al_2O_3 film grown by LPD on a GaN substrate. The film was annealed at 150°C for 2 h in an N_2 environment without any surface treatment. (a) Gaussian curve fitting of Al 2p peak and (b) Gaussian curve fitting of O 1s peak.

$$2Al(OH)_3 \rightarrow Al_2O_3 + 3H_2O$$

Results and Discussion

The GaN substrate has a transparency to He–Ne laser. Due to that, the thickness of the oxide was determined by means of the Dektak step-height measurement system through the selective deposition of oxide as shown in Fig. 1a. The GaN substrate was spin coated by photoresist, and the pattern was developed by the photolithography process, then baked at 90°C for 10 min. These patterned samples were immersed in a growth solution, and finally, the photoresist was removed by acetone. Figure 1b shows the film thickness of Al_2O_3 with deposition time at different growth temperatures. At the initial stage the deposition rate is almost linear but within 2–3 h it is nonlinear due to the nanoscale $Al(OH)_3$ colloidal particles agglomerated together to form big colloidal particles, and the deposition rate is faster. It was observed that after more than 3 h, the solution slowly started to become turbid due to the precipitation phenomenon of $Al(OH)_3$ and the pH value of the solution was decreased from 3.80 to 3.67. The slight decrease in pH value was caused by the consumption of $NaHCO_3$ in the reaction. With the addition of $NaHCO_3$ to the $Al_2(SO_4)_3$ solution, the hydrolysis of Al^{3+} particles took place, and the concentration of $Al(OH)_3$ colloid particles increased. Upon dilution of the above solution, the pH value increased to 3.80. The solubility of $Al(OH)_3$ was low near the pH value of 3.80.[11] With the progression of time the nanoscale $Al(OH)_3$ colloidal particles agglomerate together to form big colloidal particles. Due to this, the solution became turbid after more than 3 h.

Temperature was also a big factor in controlling film-growth quality and deposition rate. At a higher temperature (i.e., 40°C), film quality became poor, and the growth solution quickly became turbid. For different oxide thicknesses, the refractive index of the deposited samples varied from 1.50 to 1.65.

Figures 2a and b show the XPS of the Al 2p and O 1s core levels, respectively. For XPS, we employed monochromatic Al Kα (1486.6 eV) radiation at a power of 300 W as the excitation source and with a wide scan of 30 spectra. The take-off angle was set at 0° relative to the surface normal. The thickness of the oxide film was approximately 70 nm annealed at 150°C for 2 h without any surface treatment. The spectrum marked by a solid square showed the experimental data. Only one peak of Al 2p at a binding energy of 75.16 eV was observed. Curve fitting was done using Gaussian function (solid line) with a full width at half-maximum (fwhm) of 2.0 eV. This small fwhm value was closer to α-Al_2O_3 due to the smallest Al–Al distance.[13] In fact, aluminum has a wide range of oxides (α-Al_2O_3 and γ-Al_2O_3), namely, hydroxides $Al(OH)_3$, gibbsite, bayerite, nordstrandite, oxyhydroxides (diaspore), and γ-AlOOH (boehmite). Unfortunately, differentiating the Al 2p binding energy between different oxides, hydroxides, and oxyhydroxides by XPS was difficult, but interpreting by X-alpha calculation from

Downloaded on 2014-12-17 to IP 169.230.243.252 address. Redistribution subject to ECS terms of use (see ecsdl.org/site/terms_use) unless CC License in place (see abstract).

valance band spectra[13] was feasible. The Al 2p peak binding energy of metallic aluminum was 72.8 eV; however, no other peaks were found within the range of 65–75 eV (Al_2O_3). This indicates that Al metals were not present on the surface, as they would have resulted in a shift of the Al 2p peak toward a lower binding energy. The O 1s peak existed at 532.07 eV with a small fwhm of 2.1 eV; however, no other peaks were observed in the higher and lower binding energy sides of the O 1s region. This is due to the absence of other impurities and the impossibility of contamination in the oxide film. All data of O 1s binding energy were easily identified as similar to those of α Al_2O_3.[14] Besides, a symmetric XPS peak without shoulders and a good curve fitting by Gaussian implied that the oxide was of good chemical purity. The O/Al atomic ratio was 1.48, which was calculated by the area sensitivity factor. The survey spectrum of the surface did not show any other peaks of sodium, sulfur, gallium, and nitride. Because the solubility of $Al(OH)_3$ at the condition (pH $\sim$ 3.80) of film growth was low, the growth of Al_2O_3 thin film on a clean GaN substrate was favored. However, Na_2SO_4 was dissolved in the solution and not deposited on the substrate.

In order to investigate the effect of deposition rate and film quality[15] as well as to observe the peak binding-energy shifts by means of XPS, five different samples (A–E) with different surface pretreatments before oxide growth and with varying postannealing temperatures were used in this work.

We used two different pretreatment solutions, namely, phosphoric acid (H_3PO_4) and ammonium hydroxide (NH_4OH), as the acidic and base medium, respectively. GaN is highly stable to most chemical elements, so there is no suitable wet etchant for device fabrication. Commercially available H_3PO_4 (85%) was used in the original concentration. H_3PO_4 solution was used to remove the nitrogen-depleted layers of GaN. The damage that occurred by high-temperature annealing or the dry etching of the MOCVD of the GaN epitaxial layer grown on a *c*-plane sapphire was also removed by treatment with H_3PO_4 solution.[16] The etching rate of GaN was controlled by the hydration of the Ga ion. The *ortho* and *meta* phosphoric ions were the two attacking ions for GaN etching. The detailed mechanism of GaN etching in H_3PO_4 (85%) can be found in Ref. 17.

The surface of GaN exhibits Ga-rich phase, and Ga_2O_3 is the dominant component for surface natural oxide.[18] After NH_4OH treatment, two peaks of O–H bond[19,20] and Ga_2O_3 bond[21,22] appeared, and a significant decrease in surface natural oxide was observed. Thus, NH_4OH pretreatment is effective to create a mixed hydroxyl and oxide layer on the substrate surface, and the OH formation is favorable[15] for the growth of the oxide.

Samples A, B, and C were treated with H_3PO_4 (85%) at 80°C for 2 min. No treatment was given to sample D, while sample E was treated with a NH_4OH pH-controlled solution (pH 11.8, 25°C, 29% $NH_4OH:H_2O$ = 1:1). After the deposition of the oxide, the samples were annealed at different temperatures in a nitrogen environment. Sample A was an as-deposited oxide, sample B was thermally annealed at 600°C for 30 min, sample C was thermally annealed at 1100°C for 30 min, sample D was annealed at 150°C for 2 h, and sample E was annealed at 600°C for 30 min. All the data for oxide signals of Al 2p and O 1s peak are summarized in Table I. For all samples, the binding energy shifted toward the higher energy side due to the variation in annealing temperatures and the nonstoichiometric nature of the deposited oxide. The difference in binding energy between the core levels was almost the same for each sample, except for sample C due to a higher annealing temperature of 1100°C. Because of this, GaN remained thermally stable in the N_2 atmosphere up to 900°C. At higher temperatures, significant decomposition occurred and degraded the structural and morphological properties of the film.

Figures 3a-c show the Al 2p peak binding energy shifts of samples A, B, and C, respectively. The surface was treated by H_3PO_4 solution, and different annealing temperatures were applied. Again, we did not observe any shift in the Al 2p peak values toward a lower binding energy of metallic aluminum (72.8 eV). Figures 4a-c show the O 1s peak binding energy of samples A, B, and C, respectively. Furthermore, in samples A, B, and C, the O 1s peak 2 was found at the ranges of 527.61, 527.78, and 528.24 eV, respectively, which could be due to an impurity like the PO_4^- ion during the surface treatment before deposition or to the nonstoichiometry of Ga oxide. Significantly, we noted that the pretreatment of phosphoric acid is commonly used in strong adhesive bonding with a GaN substrate and is more resistant to attack by water vapor. Thus, we concluded from these peak results of Al 2p and O 1s that the grown film was entirely composed of amorphous Al_2O_3 film.[14] Moreover, we observed continuous binding-energy shifts among the different samples, which could be due to the native defects encountered by the change in relaxation energy of misplaced atoms and oxygen or to the aluminum vacancies. For example, there were donor states as O vacancies and acceptor states as Al vacancies. Another important observation was that the core-level peaks were shifted in the same way. The shift could be due to a change in the position of the Fermi level in the forbidden bandgap.[14] As the results show, the composition of oxide films may be attributed to Al_2O_3. However, the different pretreatment solutions did not show any noticeable change in growth rate and surface roughness.

Table I. The Al 2p, O 1s peak binding energy and fwhm of different LPD-grown Al_2O_3 on GaN samples, in which the GaN surfaces were treated by H_3PO_4, NH_4OH, and without any pretreatment, followed by different annealing temperatures.

Sample	Sample treatment and annealing temperature	O 1s Peak 1 B.E.[a] fwhm (eV)	O 1s Peak 2 B.E. (eV)	Al 2p Peak 1 B.E. fwhm (eV)	Al 2p Peak 2 B.E. (eV)
A	H_3PO_4	531.46	527.61	75.06	76.16
	As deposited	1.9		1.7	
B	H_3PO_4	531.66	527.78	75.17	76.47
	600°C, 30 min	1.9		1.7	
C	H_3PO_4	532.79	528.24	76.06	77.53
	1100°C, 30 min	2.4		1.8	
D	No surface treatment	532.07	–	75.16	–
	150°C, 2 h	2.1		2	
E	NH_4OH/H_2O(1:1)	531.79	–	75.15	75.84
	600°C, 30 min	2.18		1.78	

[a] Binding energy.

Figure 5 shows the typical Auger electron spectroscopy (AES) depth profile data for 30 nm Al_2O_3 on a GaN substrate annealed at 450°C for 30 min in N_2 atmosphere. The AES data revealed that the composition of aluminum (Al) and oxygen (O) atoms in oxide film was uniform from the surface to the oxide-semiconductor interface. Small gallium (Ga) outdiffusion from the GaN substrate and Al indiffusion into the GaN region during alumina thin-film deposition was also observed. The films were nearly stoichiometric, with an approximately constant composition of Al and O atoms from the bulk to the interface. This result also confirms a good interface with Al and O as well as the absence of peaks in the interface region. Figure 6 displays the surface morphologies of oxides on GaN for different annealing temperatures. The atomic force microscopy (AFM) data (the scan rate was 1.3 Hz and the set point was 0.158 V) shows that the root-mean-square (rms) surface roughness of a 50 nm thick Al_2O_3 film was (height modulation in the 2 $\times$ 2 μm^2) only 1.025 nm after high-temperature annealing at 750°C, which was low as compared to SiO_2 on a GaN substrate (5.2 nm).[9] The surface morphology was improved after high-temperature annealing. Therefore, this smooth-surface result provides potential for GaN MOS-HEMT device applications.

Downloaded on 2014-12-17 to IP 169.230.243.252 address. Redistribution subject to ECS terms of use (see ecsdl.org/site/terms_use) unless CC License in place (see abstract).

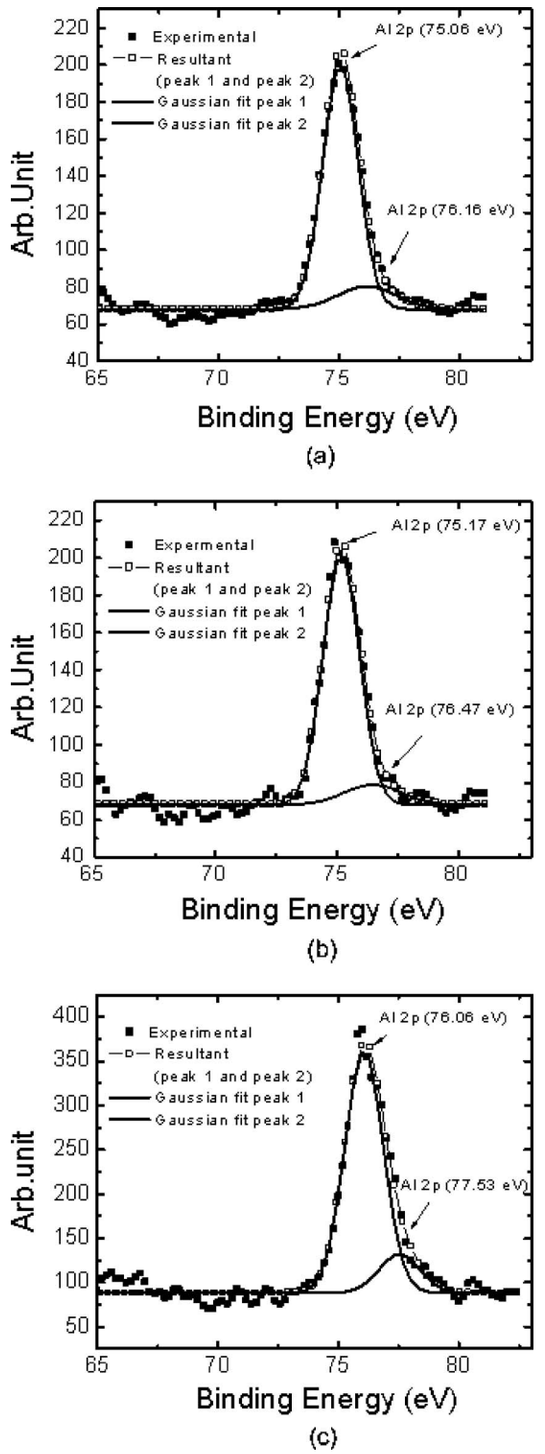

Figure 3. Al 2p peak binding energy shifts; the surface was treated by H_3PO_4 solution following different annealing temperatures. (a) Sample A was as-deposited, (b) sample B was annealed at 600°C for 30 min, and (c) sample C was annealed at 1100°C for 30 min.

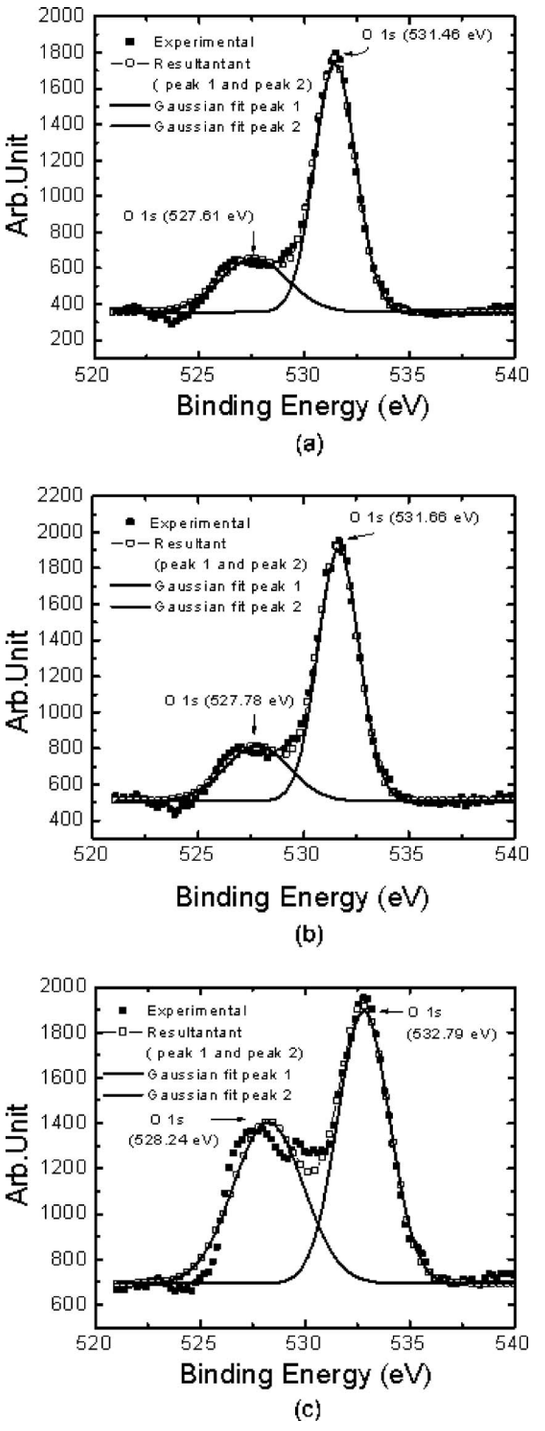

Figure 4. O 1s peak binding energy shifts; the surface was treated by H_3PO_4 solution following different annealing temperatures. (a) Sample A was as-deposited, (b) sample B was annealed at 600°C for 30 min, and (c) sample C was annealed at 1100°C for 30 min.

All these results indicate that the good physical and chemical quality of Al_2O_3 films can be properly deposited on GaN substrates by the LPD process.

For the investigation of electrical properties of the oxide film, a device structure made of MOS diodes was employed. The Si-doped n-type GaN epitaxial layer grown on a *c*-plane sapphire substrate with a carrier concentration of 1×10^{18} cm^{-3} was used as the substrate to measure the leakage current density. The procedures for fabrication of the device were as follows. To form the ohmic contacts, a Ti/Al layer was deposited by sputtering, followed by a 30 s rapid thermal annealing at 900°C in nitrogen atmosphere. Then Al_2O_3 oxide film was grown on the substrate. Finally, Al metal pads were evaporated on the oxide as anodic plates with an area of

Downloaded on 2014-12-17 to IP 169.230.243.252 address. Redistribution subject to ECS terms of use (see ecsdl.org/site/terms_use) unless CC License in place (see abstract).

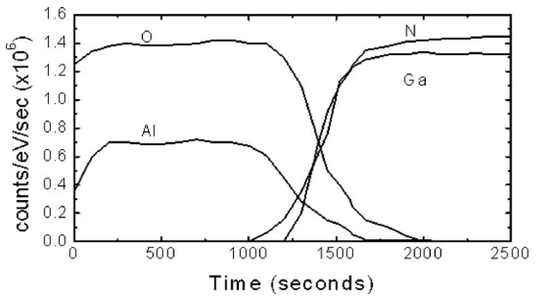

Figure 5. Typical AES depth profiles of an aluminum oxide film deposited on a GaN substrate.

1–7 × 10^{-5} cm^2. Figure 7a shows the typical leakage current density of LPD-grown Al_2O_3 thin film on GaN annealed at 150°C for 30 min. At a negative electric field of 1 MV/cm, the corresponding leakage current densities ranged from 10^{-4} to 10^{-5} A/cm^2. The breakdown electric field was more than 10 MV/cm for a 50 nm oxide thickness. Furthermore, the leakage current density could be improved by a high-temperature annealing of oxide films. Figure 7b shows the improvement of leakage current density with a higher annealing temperature in N_2 ambient. After annealing at 750°C, the leakage current density was reduced to the order of 10^{-6}–10^{-7} A/cm^2 at a negative electric field of 1 MV/cm. This leakage current density of thin Al_2O_3 film on GaN was quite comparable to or better than that of SiO_2 on GaN[9] and Al_2O_3 on Si by sputtering.[23] However, the result shows that the breakdown field was higher. Electronic conduction may occur within the oxides via hopping transport or tunneling process between trap sites, which may be caused by unattached bonding (defects), porous structures (pinholes), or impurities. As a result, pinhole-free insulating oxides have better electrical insulating properties such as lower leakage currents and higher breakdown fields.[24] The capacitance-voltage (*C-V*) characteristics yielded the bulk and interface defect densities of the oxide. Figure 8 shows the typical *C-V* characteristics measured by 4280 A at frequency 1 MHz, exhibiting the GaN surface-charge regimes of electron accumulation, depletion, and inversion. At positive dc bias applied to the top Al gate terminal, the net capacitance equaled the oxide capacitance C_{ox} due to the accumulation of electrons at the n-type GaN surface. In the case when moderate negative voltage is applied to the top gate, a positive space-charge region is induced in the n-type semiconductor. By implying a sufficiently

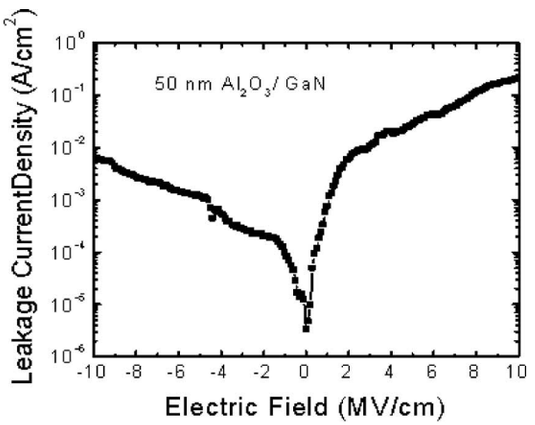

(a)

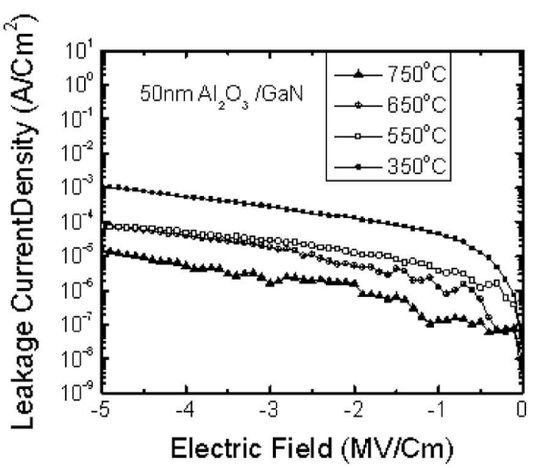

(b)

Figure 7. (a) The log *I-V* characteristics for the 50 nm thick Al_2O_3 on GaN annealed at 150°C for 30 min. (b) The improvement of leakage current densities with varying annealing temperatures.

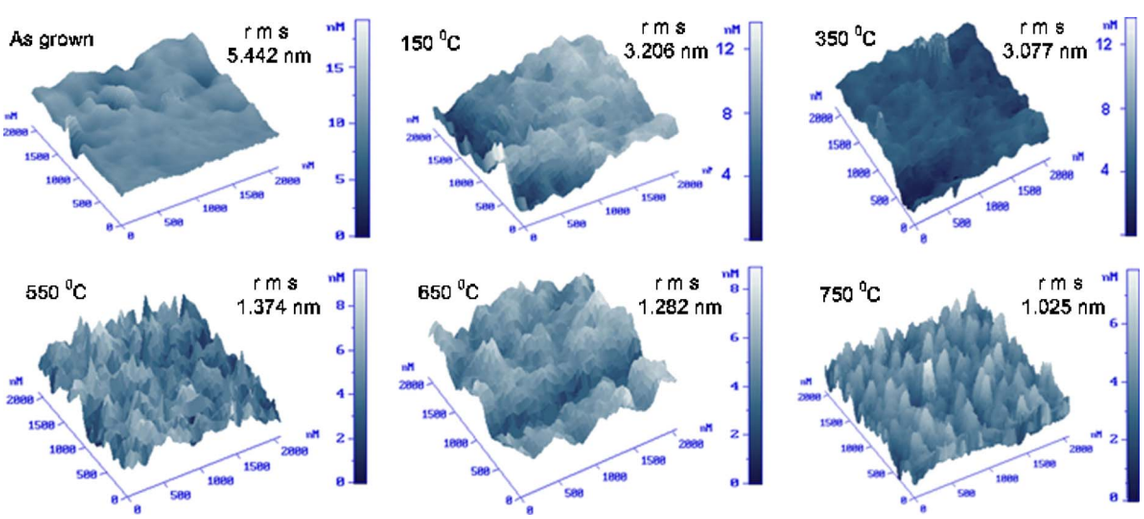

Figure 6. (Color online) AFM (3D image) surface morphology of Al_2O_3 oxide deposited on a GaN substrate for different annealing temperatures in N_2 ambient for 30 min.

Downloaded on 2014-12-17 to IP 169.230.243.252 address. Redistribution subject to ECS terms of use (see ecsdl.org/site/terms_use) unless CC License in place (see abstract).

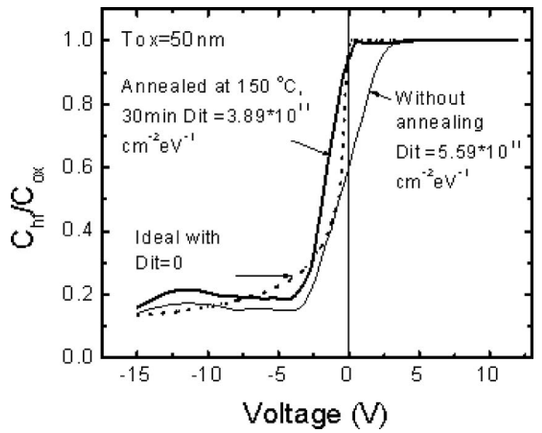

Figure 8. The measured and ideal *C-V* characteristics at 1 MHz. The calculated interface trap densities were 3.89×10^{11} cm^{-2} eV^{-1} for an oxide thickness of 50 nm on GaN annealed at 150°C (30 min) and 5.59×10^{11} cm^{-2} eV^{-1} for as-grown oxide.

large negative voltage to the gate of the MOS capacitor, an inversion layer of holes was induced at the oxide-semiconductor interface. The thin line and thick solid lines in Fig. 8 represent the experimental results of the as-grown and annealed films at 150°C for 30 min in N_2 ambient, respectively. The approximate curve of ideal *C-V* characteristics based on theoretical calculation is also shown in broken lines. According to the high-frequency (Terman's) method,[25] the distortion of the *C-V* curves is caused by a high charge density at the interface. Obviously, there was a lower interface charge density for the annealed oxide film than that for the as-grown film. The interface charge density (D_{it}) and flatband voltage (V_{FB}) can be determined by employing the equation $D_{it} = C_{ox}/q\ [(d\phi_s/dV)^{-1} - 1] - C_D/q$, where C_{ox} and C_D are the oxide and depletion capacitance, respectively. The surface potential (ϕ_s) is the potential difference across the space-charge layer. At $\phi_s = 0$, the applying bias voltage represents the V_{FB}. A higher slope value is responsible for a lower state density. According to the plot and calculated results, the V_{FB} was +2 and +0.2 V for the as-grown and annealed samples, respectively. The calculated interface trap densities were 3.89×10^{11} cm^{-2} eV^{-1} for an oxide thickness of 50 nm annealed at 150°C (30 min) and 5.59×10^{11} cm^{-2} eV^{-1} for the as-grown oxide film. Thus, after annealing, the average D_{it} near the midgap of the LPD-grown oxide was reduced from 5.59 to 3.89×10^{11} cm^{-2} eV^{-1}. In addition, the *C-V* characteristics in the accumulation region exhibited an almost completely horizontal curve, which showed that the leakage current of the oxide was low enough to accumulate majority carriers. According to the measured capacitance at a dc bias voltage under accumulation, the calculated relative permittivity (ε_r) of oxide was 9.7 for the sample annealed at 450°C. To estimate the (ε_r), we applied the equation $C_{measured} = \varepsilon_r \varepsilon_o (A/t_{ox})$, where A is the area of the anodic plate of the capacitors, $t_{ox} = 50$ nm is the oxide thickness, and $C_{measured} = 12$ pF. The estimated figure is close to the value of the dielectric constant (10.6) of sapphire (α-Al_2O_3).[26]

As these results show, the proposed method is likely to have the potential to achieve a high gate breakdown voltage and low interface trap charge density for GaN MOSHEMT device applications.

Conclusion

In summary, we have achieved a low-cost, more efficient, and low-temperature (~30°C) liquid-phase deposition of Al_2O_3 thin films on GaN (deposition rate of 35 nm/h). The XPS study of LPD Al_2O_3/GaN with and without H_3PO4 and NH_4OH pretreatments were investigated in order to observe the shift in peak binding energy. Different samples did not show significant shifts in the peak binding energy of Al 2p (75 eV) and O 1s (532 eV) core levels. The good quality of alumina thin films was obtained by optimization of $Al_2(SO4)_3 = 0.0834$ mol/L and $NaHCO_3 = 0.211$ mol/L concentrations. The refractive index and relative permittivity of oxide were 1.63 and 9.7, respectively. The various analytical results through XPS, AES, and AFM showed that a reliable and good-quality aluminum oxide film could be obtained. Moreover, the results showed that in terms of leakage current density, breakdown electric field, and interface trap charge density, this LPD-Al_2O_3/GaN method provides a unique opportunity to make high-quality gate dielectrics for GaN MOSFET applications.

Acknowledgments

This work was supported in part by the National Science Council under contract no. NSC94-2215-E-006-001 and NSC95-2221-E-428-MY3 by the Ministry of Education Program for Promoting Academic Excellence of Universities under grant no. A-91E-FA08-1-4, and by the Foundation of Chen under the Jieh-Chen Scholarship of Tainan, Taiwan.

National Cheng-Kung University assisted in meeting the publication costs of this article.

References

1. R. A. Abbott and T. I. Kamins, *Solid-State Electron.*, **13**, 565 (1970).
2. G. D. Wilk, R. M. Wallace, and J. M. Anthony, *J. Appl. Phys.*, **89**, 5243 (2001).
3. K. P. Pande, V. K. R. Nair, and D. Gutierrez, *J. Appl. Phys.*, **54**, 5436 (1983).
4. J. Kolodzey, E. A. Chowdhury, T. N. Adam, G. Qui, I. Rau, J. O. Olowolafe, J. S. Suehle, and Y. Chen, *IEEE Trans. Electron Devices*, **47**, 121 (2000).
5. J. S. Kim, H. A. Marzouk, P. J. Reucroft, J. D. Robertson, and C. E. Hamrin, Jr., *Appl. Phys. Lett.*, **62**, 681 (1993).
6. M. Voigt and M. Sokolowski, *Mater. Sci. Eng., B*, **109**, 99 (2004).
7. P. Tristant, Z. Ding, Q. B. Trang, V. H. Hidalgo, J. L. Jauberteau, J. Desmaison, and C. Dong, *Thin Solid Films*, **390**, 51 (2001).
8. H. C. Lin, P. D. Ye, and G. D. Wilk, *Appl. Phys. Lett.*, **87**, 182904 (2005).
9. H. R. Wu, K. W. Lee, T. B. Nian, D. W. Chou, J. J. Huang Wu, Y. H. Wang, M. P. Huang, P. W. Sze, Y. K. Su, S. J. Chang, C. H. Ho, C. I. Chiang, Y. T. Chern, F. S. Juang, T. C. Wen, W. I. Lee, and J. I. Chyi, *Mater. Chem. Phys.*, **80**, 329 (2003).
10. J. Sun, L. H. Hu, Z. Y. Wang, and G. T. Du, *Mater. Sci. Forum*, **475-479**, 1725 (2005).
11. D. F. Shriver, P. W. Atkins, and C. H. Langford, *Inorganic Chemistry*, Chap. 5, p. 164, Oxford University Press, New York (1990).
12. Z. D. Zivcovic and B. Dobovisek, *J. Therm. Anal.*, **12**, 207 (1977).
13. S. Thomas and P. M. A. Sherwood, *Anal. Chem.*, **64**, 2488 (1992).
14. W. M. Mullins and B. L. Averbach, *Surf. Sci.*, **206**, 52 (1988).
15. M. P. Houng, C. J. Huang, Y. H. Wang, N. F. Wang, and W. J. Chang, *J. Appl. Phys.*, **82**, 5788 (1997).
16. B. J. Kim, J. W. Lee, H. S. Park, Y. Park, and T. I. Kim, *J. Electron. Mater.*, **27**, 5 (1998).
17. A. Shintani and S. Minagawa, *J. Electrochem. Soc.*, **123**, 706 (1976).
18. T. Hashizume, S. Ootomo, S. Oyama, M. Konishi, and H. Hasegawa, *J. Vac. Sci. Technol. B*, **19**, 1675 (2001).
19. I. Waki, H. Fujioka, K. Ono, M. Miki, and A. Fukizawa, *Jpn. J. Appl. Phys., Part 1*, **39**, 4451 (2000).
20. Y. J. Lin and C. T. Lee, *Appl. Phys. Lett.*, **77**, 3986 (2000).
21. G. Hollinger, S. Skheyta-Kabbani, and M. Gendry, *Phys. Rev. B*, **49**, 11159 (1994).
22. N. J. Watkins, G. W. Wicks, and Y. Gao, *Appl. Phys. Lett.*, **75**, 2602 (1999).
23. J. Kolodzey, E. A. Choudhary, T. N. Adam, G. Qui, I. Rau, J. O. Olowolafe, J. S. Suehle, and Y. Chen, *IEEE Trans. Electron Devices*, **47**, 121 (2000).
24. *Physics and Chemistry of III-V Compound Semiconductor Interfaces*, C. W. Wilmsen, Editor, Chap. 3, Plenum Press, New York (1985).
25. E. H. Nicolian and J. R. Brews, *MOS (Metal Oxide Semiconductor) Physics and Technology*, Chap. 8, John Wiley & Sons, Inc., New York (1982).
26. *Handbook of Thin Film Technology*, L. I. Maissel and R. Glang, Editors, p. 6.12, McGraw-Hill, New York (1983).

Downloaded on 2014-12-17 to IP 169.230.243.252 address. Redistribution subject to ECS terms of use (see ecsdl.org/site/terms_use) unless CC License in place (see abstract).